

A Study of NanoParticles of Gamma Irradiated Zinc Oxide and Its Antibacterial effect on *Klebsiella pneumonia* and *Pseudomonas aeruginosa*

Swaroop K.¹, Sana Sheikh², Chandrashekar K. R.², and Somashekarappa H. M.^{1*}

¹Centre for Application of Radioisotopes and Radiation Technology (CARRT), Mangalore University, Mangalagangothri – 574 199, Karnataka, India

²Department of Applied Botany, Mangalore University, Mangalagangothri-574 199, Karnataka, India

Abstract: This study carries out the assessment of the antibacterial activity of zinc oxide (ZnO) nanoparticles synthesized with various dosages of the gamma radiations on *Klebsiella pneumonia* (*K pneumonia*) and *Pseudomonas aeruginosa* (*P aeruginosa*) bacteria. Additionally, there is the synthesis of the ZnO nanoparticles using the combustion technique, and the samples that were synthesized were then irradiated with gamma radiation of various dosages from 0 to 200 kGy. The characteristics of all of the samples in the study were by the use of Powder X-ray Diffractometer (Powder XRD), Fourier Transform Infrared Spectrometer (FTIR), Ultraviolet-Visible Spectrophotometer (UV-Vis), and Field Emission Scanning Electron Microscopy (FESEM).

Keywords – Antibacterial, Gamma irradiation, SEM, XRD, Zinc oxide.

I. Introduction

Transition metal oxides have a wide range of applications as catalysts, sensors, superconductors, antimicrobial agents, etc. Among transition metal oxides, zinc oxide (ZnO) nanoparticles are of special interest because of its large exciton binding energy of 60 meV with a direct band gap of 3.37 eV [1-3]. It has been widely used in gas sensors, transparent conductors, piezoelectric application, and as antimicrobial agents. Nanocrystalline powders, due to their average particle size of less than 100 nm may show different behaviours resulting from higher surface energy due to the large surface area and the wide gap between the valence band and the conduction band [4]. These phenomena may increase the potential use of the material including its optical, chemical, and electromagnetic properties [5, 6].

Researchers have extensively studied the role of noble metals such as gold and silver nanoparticles as antimicrobial agents [7-9]. Recently, the antimicrobial activity of nano-sized ZnO particles has attracted attention [10, 11], since the small size (less than 100 nm) and high surface to volume ratio of the nanoparticles allow for better interaction with bacteria [10, 12]. Recent studies have shown that these nanoparticles have selective toxicity to bacteria and exhibit minimal effects on human cells [13, 14]. Since, most of the ZnO nanoparticles are produced synthetically; it has certain advantages, compared to silver nanoparticles, such as lower cost and white appearance [13].

Ionizing radiations have been reported to modify surface structure, texture, electric, and magnetic properties of a wide variety of solids [15, 16]. Extensive studies have been carried out by researcher on the antimicrobial activity of ZnO [17], but studies on the antimicrobial activity of ZnO nanomaterials subjected to gamma irradiation are sparse. In the present study, solution combustion technique has been employed to synthesize ZnO nanoparticles. The synthesized ZnO nanoparticles were treated with gamma radiation with doses ranging from 0 to 200 kGy, and antibacterial studies were carried out using gram negative *Klebsiella pneumonia* (*K pneumonia*) and *Pseudomonas aeruginosa* (*P aeruginosa*) bacterial cultures.

II. Materials and Methods

1.1 Preparation of ZnO nanoparticles

Zinc nitrate hexahydrate [Zn(NO₃)₂·6H₂O] (Himedia, Mumbai, India) as an oxidizing agent and glycine (Merck, Mumbai, India) as fuel were used for synthesizing ZnO nanoparticles. All the chemical reagents used in

synthesizing the ZnO nanoparticles were used directly without any further purification. MilliQ water was used as a solvent throughout the experiment.

The molar ratio of oxidant-to-fuel was fixed to 1:1, and the aqueous solution taken in a borosilicate glass container was heated to 400° C in a muffle furnace. The solution is boiled to form the foams, and undergoes flameless combustion to produce ZnO nanoparticles in powdered form. This method is based on the principle that once a reaction is initiated by heating, an exothermic reaction occurs that becomes self-sustaining within a certain time interval, resulting in a powder form as the final product.

1.2 Gamma irradiation

The gamma irradiation process was carried out using the Gamma Irradiator (GC5000, BRIT, India) which has cobalt-60 (⁶⁰Co) as a radioactive source and delivered a dose rate of about 7.23 kGy/hr at the time of irradiation. The synthesized ZnO powder samples was divided into four replicates and sealed in plastic tubes. The samples were irradiated for different doses of gamma radiation from 0 to 200 kGy (Table 1). Irradiation of the samples was conducted at room temperature and in the presence of air.

1.3 Antibacterial study of ZnO nanoparticles

Two species of gram negative [*Pseudomonas aeruginosa* (NCIM 2200), *Klebsiella pneumonia* (NCIM 2957) procured from the National Chemical Laboratory, Pune, India] bacteria were used for the microbial sensitivity assay studies.

The disk diffusion method was employed for the antibacterial assay studies. In vitro antibacterial activity was studied by taking two hundred micro liters of overnight grown cultures of each organism and dispensed in 20 ml of sterile nutrient broth and incubated for 4-5 hours at 37° C to standardize the culture to 10⁻⁵ CFU/ml. For this, 0.1 ml (10⁻⁵ CFU /ml) of 24 hr old bacterial culture was placed on the Muller Hinton agar medium and spread throughout the plate by spread plate technique [18].

Each set of the synthesized ZnO nanoparticles was dispersed (30 µg/L) in dimethyl sulfoxide (DMSO) using ultra-sonicator for 5 min and loaded on to sterile discs (250µg concentration, 6 mm diameter) purchased from HIMEDIA laboratories, individually and aseptically before screening for antibacterial activity. The antibacterial activity was recorded by measuring the diameter zone of inhibition. Streptomycin and DMSO were used as positive and negative controls against the bacterial strains, respectively.

1.4 Characterization of ZnO nanoparticles

The crystallite size and structural information were recorded by powder X-ray diffraction (Rigaku Miniflex) using Cu Kα radiation (1.5406 Å). The intensity data was collected for all the samples over a 2θ range of 25-80° with a scan speed of 3° per min. The average grain size of the samples was estimated with the help of Scherrer equation (1) using the diffraction intensity of (101) peak.

$$d = \frac{0.89 \lambda}{\beta \cos \theta} \dots\dots\dots (1)$$

Where, λ is the wavelength (Cu Kα), β is the full width at the half- maximum (FWHM) of the ZnO (101) peak, and θ is the diffraction angle.

The lattice strain (ε_{av}) has been calculated using tangent formula (equation 2).

$$\epsilon_{av} = \frac{\beta}{4 \tan \theta} \dots\dots\dots (2)$$

The optical absorption spectrum was taken using the UV-Vis spectrophotometer (Shimadzu, UV-1800) in aqueous condition within the wavelength range of 250 to 600 nm. The energy band gap (E_g) values of the samples were calculated using the equation 3.

$$E_g = \frac{hc}{\lambda_m} \text{ eV} \dots\dots\dots (3)$$

Where, h is the planks constant, c is the speed of light and λ_m is the wavelength corresponding to maximum wavelength.

The elemental constituents of the material and various functional groups present in the material were analyzed using FTIR (Prestige 21, Shimadzu, Japan) in the wavelength range of 400-4000 cm⁻¹.

The surface morphology of all the samples was studied using the Field Emission Scanning Electron Microscopy (ULTRA 55 FESEM, Karl Zeiss) at 1 µm range with uniform magnification.

III. Results and Discussion

The powder XRD pattern of the samples is shown in Fig. 1. All the peaks match with the ZnO hexagonal wurtzite structure of JCPDS standards. There are no other characteristic impurity peaks present. This confirms that the products obtained are in the pure phase. The crystallite size for irradiated and un-irradiated samples were calculated using equation 1 ranges from 13 to 16 nm. The lattice strain (ϵ_{av}) has been calculated using equation 2, which shows significant increase in the lattice strain associated with the reduction of crystallite size of ZnO. The spectra presented in Fig. 1 shows no structural variation among the irradiated and un-irradiated samples. A detailed analysis of the XRD is presented in Table 1.

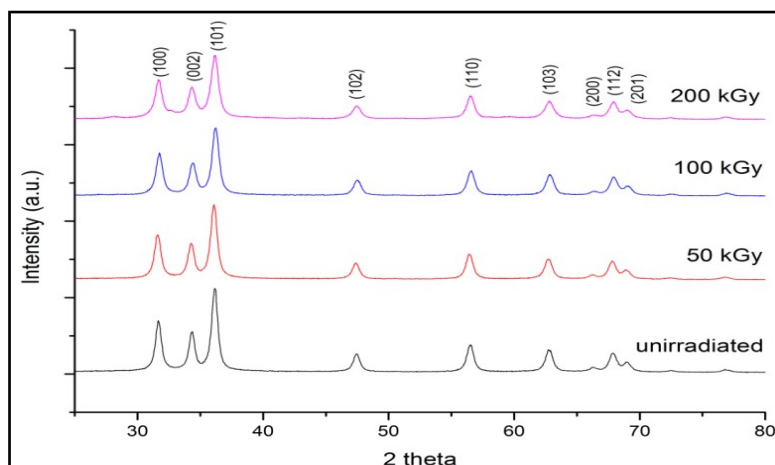


Figure 1: Powder XRD pattern of un-irradiated and irradiated ZnO synthesized by solution combustion technique

Table 1: Variation in the crystallite size, lattice strain, and energy band gap of ZnO nanoparticles irradiated from 0 to 200 kGy

Sample	Crystallite size 'd' in nm	Lattice strain ' ϵ_{av} '	Wavelength corresponds to maximum absorption (λ_m) in nm	Energy band gap (E_g) in eV
Un-irradiated	16	0.4928	369	3.3668
50 kGy	14.5	0.4619	363	3.4225
100 kGy	13.5	0.4515	360	3.4510
200 kGy	12.9	0.4264	358	3.4703

The UV-Vis absorption spectrum of ZnO nanoparticles are shown in Fig. 2. All the samples exhibits strong absorption peaks at about 358 to 369 nm. From the optical absorption spectra (Fig. 2) it is clear that the absorption edge of gamma irradiated samples symmetrically shifts towards the lower wavelength or higher energy region with respect to un-irradiated sample. The energy band gap (E_g) of all the samples were calculated using equation 3 and tabulated in Table 1. The appearance of sharp excitonic peak indicates the high crystalline quality of the grown nanostructures.

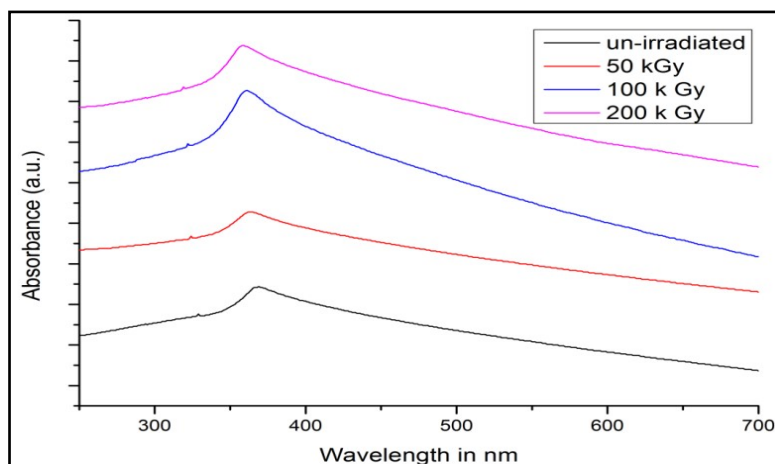


Figure 2: UV-Vis spectroscopic analysis of un-irradiated and irradiated ZnO nanoparticles

Fig. 3 shows the FTIR spectra of the ZnO nanoparticles irradiated for gamma irradiation dose from 0 to 200 kGy. The peak observed at ~ 3470 and ~ 1030 cm^{-1} may be due to O-H stretching and deforming, probably due to atmospheric moisture [19]. The strong absorption peak at ~ 470 cm^{-1} represents the Zn-O stretching frequency [20, 21].

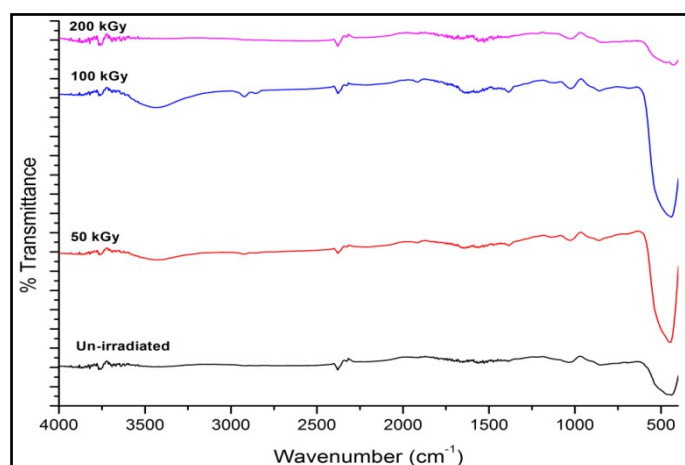


Figure 3: FTIR analysis showing the functional groups involved in the prepared samples.

Fig. 4 shows the SEM images of nanocrystalline ZnO. The SEM image of the pure ZnO powder exhibits high porosity, which is attributed to the release of gaseous products like H_2O , CO_2 , and N_2 during the combustion process [22, 23]. The SEM images show a progressive increase in porosity with increase of gamma radiation dose. The maximum increase corresponds to maximum dose 200 kGy as can be seen from image 4 (d). The increase in porosity was noticed in the irradiated samples in comparison to the un-irradiated samples.

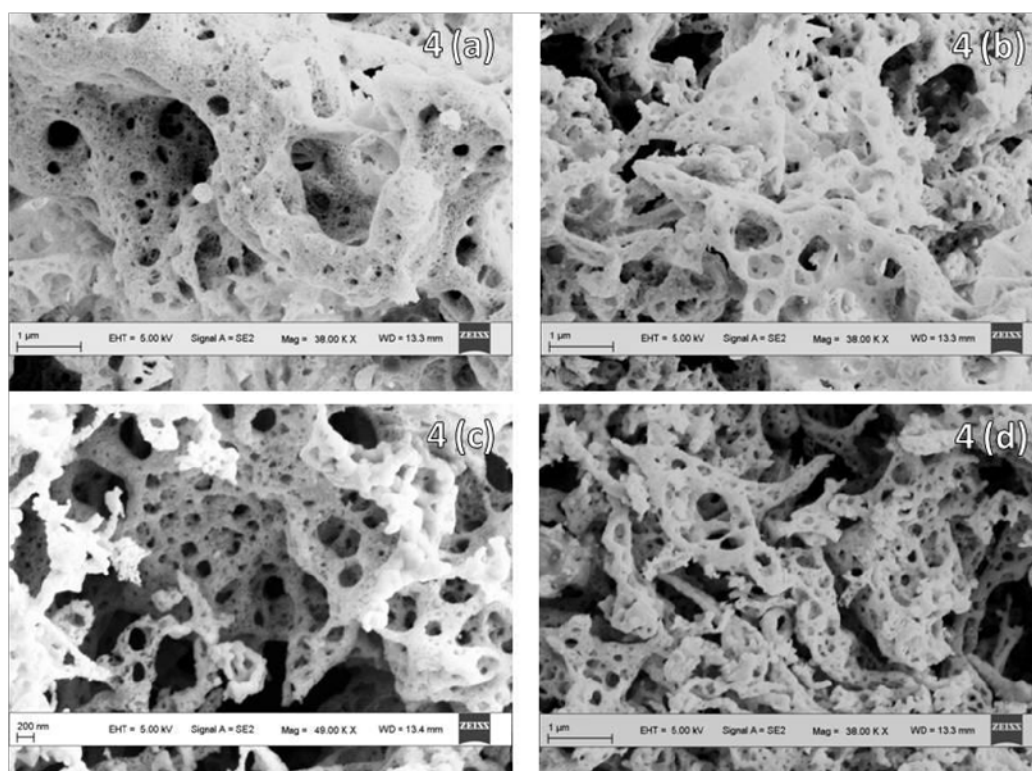


Figure 4: Comparison of SEM images of ZnO nanoparticles irradiated with different dosages (a) Unirradiated, (b) 50 kGy, (c) 100 kGy, and (d) 200 kGy

The antibacterial activity of ZnO nanoparticles was assessed by agar disk diffusion method in order to investigate the efficacy of the gamma irradiation on the gram negative bacteria namely, *K pneumonia* and *P aeruginosa*. It has been observed from Fig. 5 and Table 2 that the zone of inhibition increased significantly from

8.5 mm to 16.5 mm and 10 mm to 18 mm in the case of *K pneumonia* and *P aeruginosa*, respectively with the increase of the gamma radiation dose. In both cases, gamma irradiation has led to the enhancement of the inhibition zone, from 50 kGy to 200 kGy. DMSO, which was used as a negative control did not show any activity, whereas the positive control, streptomycin showed maximum activity against both bacteria. Fig. 6 shows the succeeding increase in the antibacterial activity with increase in gamma irradiation dose.

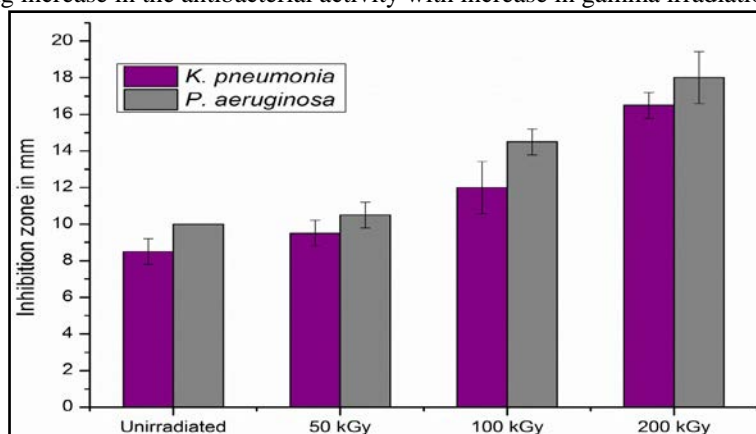


Figure 5: Graph showing increase in inhibition zone with respect to gamma irradiation dose for *K pneumonia* and *P aeruginosa*

Table 2: Antibacterial assessment of *K pneumonia* and *P aeruginosa* by disk diffusion method

Sample	Mean value of inhibition zone in mm	
	<i>Klebsiella pneumonia</i>	<i>Pseudomonas aeruginosa</i>
Un-irradiated	8.5 ± 0.7	10 ± 0
50 kGy	9.5 ± 0.7	10.5 ± 0.7
100 kGy	12 ± 1.41	14.5 ± 0.7
200 kGy	16.5 ± 0.7	18 ± 1.41

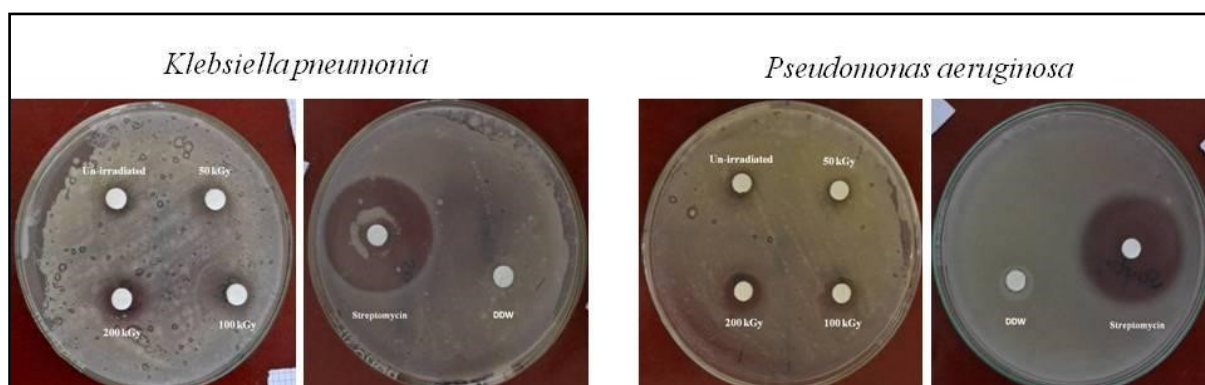


Figure 6: Antibacterial activity images of gamma irradiated ZnO nanoparticles against *K pneumonia* and *P aeruginosa*

IV. Conclusion

The structural, optical, functional groups and morphology of gamma irradiated ZnO nanoparticles synthesized by the solution combustion method has been investigated. The antibacterial activity of gamma irradiated ZnO nanoparticles against gram negative bacterium, *K pneumonia* and *P aeruginosa* are reported. The XRD results showed that ZnO nanoparticles were composed of hexagonal wurtzite structure with very good crystallinity, which has not been altered by the gamma irradiation treatment. The average particle size (d) decreased with increase in gamma irradiation dose. The FTIR studies confirm the characteristic peaks at $\sim 470 \text{ cm}^{-1}$ for Zn-O stretching and also the absence of any major impurities in the samples. Uv-vis analysis shows substantial increase in the energy band gap (E_g) with respect to gamma irradiation dose. SEM images confirm the porous nature of all the samples which tend to increase with the increase of gamma radiation dose. The current work indicates that gamma irradiation has led to increase in the surface area which in turn has resulted in the increase in the antibacterial activity of *P aeruginosa* and *K pneumonia* bacterial culture, and the antibacterial activity was closely related to the surface area of the ZnO nanoparticles [24].

Acknowledgements

Authors are thankful to the Coordinator, DST-PURSE programme, Mangalore University for permitting to use FESEM facility and the Chairman, Department of Physics, Mangalore University for XRD facility under DST-FIST programme.

References

- [1] Z. Ibupoto, K. Khun, M. Eriksson, M. AlSalhi, M. Atif, A. Ansari, and M. Willander, Hydrothermal growth of vertically aligned ZnO nanorods using a biocomposite seed layer of ZnO nanoparticles, *Materials*, 6(8), 2013, 3584-3597.
- [2] S. Hussain, Y. Khan, V. Khranovskyy, R. Muhammad, R. Yakimova, Effect of oxygen content on the structural and optical properties of ZnO films grown by atmospheric pressure MOCVD, *Progress in Natural Science: Materials International*, 23(1), 2013, 44-50.
- [3] Z. Bai, X. Yan, X. Chen, K. Zhao, P. Lin, Y. Zhang, High sensitivity, fast speed and self-powered ultraviolet photodetectors based on ZnO micro/nanowire networks, *Progress in Natural Science: Materials International*, 24, 2014, 1-5.
- [4] Y. T. Prabhu, K. V. Rao, V. Seshu, S. Kumar, B. S. Kumari, Synthesis of ZnO Nanoparticles by a novel surfactant assisted amine combustion method, *Advances in Nanoparticles*, 2, 2013, 45-50.
- [5] R. Srivastava, Investigation on temperature sensing of nanostructured zinc oxide synthesized via oxalate route, *Journal of Sensor Technology*, 2, 2012, 8-12.
- [6] A. Kopp Alves, C. P. Bergmann, F. A. Berutti, Novel synthesis and characterization of nanostructured materials, *Engineering Materials*, 3, 2013, 11-22.
- [7] L. Vayssieres, On the design of advanced metal oxide nanomaterials, *International Journal of Nanotechnology*, 1(1), 2004, 1-40.
- [8] Pallab Sanpui, A. Murugadoss, P. V. Durga Prasad, Siddhartha Sankar Ghosh, Arun Chattopadhyay, The antibacterial properties of a novel chitosan-Ag-nanoparticle composite, *International Journal of Food Microbiology*, 124, 2008, 142-146.
- [9] L. R. Jaidev, G. Narasimha, Fungal mediated biosynthesis of silver nanoparticles, characterization and antimicrobial activity, *Colloids and Surfaces B: Biointerfaces*, 81, 2010, 430-433.
- [10] P. Taylor, K. B. Sapnar, L. A. Ghule, A. Bankar, S. Zinjarde, and V. N. Bhoraskar, Antimicrobial activity of 6.5 MeV electron irradiated ZnO nanoparticles synthesized by microwave-assisted method, *International Journal of Green Nanotechnology*, 4, 2012, 477-483.
- [11] S. Azizi, M. Ahmad, M. Mahdavi, and S. Abdolmohammadi, Preparation, characterization, and antimicrobial activities of ZnO nanoparticles/cellulose nanocrystal nanocomposites, *Bio Resources*, 8, 2013, 1841-1851.
- [12] M. Saadat, S. R. Mohammadi, M. Eskandari, Evaluation of antibacterial activity of ZnO and TiO₂ nanoparticles on planktonic and biofilm cells of *Pseudomonas aeruginosa*, *Biosciences Biotechnology Research Asia*, 10(2), 2013, 629-635.
- [13] S. Nagarajan, K. Arumugam Kuppasamy, Extracellular synthesis of zinc oxide nanoparticle using seaweeds of gulf of Mannar, India, *Journal of Nanobiotechnology*, 11, 2013, 1-11.
- [14] G. Singh, E. M. Joyce, J. Beddow, T. J. Mason, Evaluation of antibacterial activity of ZnO nanoparticles, *Journal of Microbiology, Biotechnology and Food Sciences*, 2, 2012, 106-120.
- [15] S. A. El-molla, S. A. Ismail, M. M. Ibrahim, Effect of gamma irradiation and aging on surface and catalytic activity of nanosized CuO/MgO system, *Journal of Mexican Chemical Society*, 55(3), 2011, 154-163.
- [16] L. Zhang, Y. Ding, M. Povey, D. York, ZnO nanofluids – a potential antibacterial agent, *Progress in Natural Science: Materials International*, 18, 2008, 939-944.
- [17] S. Gunalan, R. Sivaraj, V. Rajendran, Green synthesised ZnO nanoparticles against bacterial pathogens, *Progress in Natural Science: Materials International*, 22, 2012, 693-700.
- [18] Performance Standards for Antimicrobial Disk and Dilution Susceptibility Tests for Bacteria Isolated from Animals □; Approved
Standard — Second Edition, 22, no. 6.
- [19] H. Kumar, R. Rani, Structural and optical characterization of ZnO nanoparticles synthesized by microemulsion route, *International Letters of Chemistry, Physics and Astronomy*, 14, 2013, 26-36.
- [20] Z. R. Khan, Opticle and structural properties of ZnO thin films fabricated by sol gel method, *Material Sciences and Applications*, 2, 2011, 340-345.
- [21] R. N. Gayen, K. Sarkar, S. Hussain, R. Bhar, and A. K. Pal, ZnO films prepared by modified sol gel technique, *Indian Journal of Pure Applied Physics*, 49, 2011, 470-477.
- [22] M. L. Dinesha, H. S. Jayanna, S. Ashoka, and G. T. Chandrappa, Effect of Fe doping concentration on electrical and magnetic properties of ZnO nanoparticles prepared by solution combustion method, *Journal of Optoelectronics and Advanced Materials*, 11, 2009, 964-969.
- [23] V. Chandore, G. Carpenter, R. Sen, N. Gupta, Synthesis of nano crystalline ZnO by microwave assisted combustion method, *International Journal of Environmental Sciences*, 4, 2013, 45-47.
- [24] B. Vatsha, P. Tetyana, P. M. Shumbula, J. C. Ngila, L. M. Sikhwivhilu, R. M. Moutloali, Effect of precipitation temperature on nanoparticle surface area and antibacterial behaviour of Mg(OH)₂ and MgO nanoparticles, *Journal of Biomedical Nanotechnology*, 4, 2013, 365-373.